

# RSC Advances



This is an *Accepted Manuscript*, which has been through the Royal Society of Chemistry peer review process and has been accepted for publication.

*Accepted Manuscripts* are published online shortly after acceptance, before technical editing, formatting and proof reading. Using this free service, authors can make their results available to the community, in citable form, before we publish the edited article. This *Accepted Manuscript* will be replaced by the edited, formatted and paginated article as soon as this is available.

You can find more information about *Accepted Manuscripts* in the [Information for Authors](#).

Please note that technical editing may introduce minor changes to the text and/or graphics, which may alter content. The journal's standard [Terms & Conditions](#) and the [Ethical guidelines](#) still apply. In no event shall the Royal Society of Chemistry be held responsible for any errors or omissions in this *Accepted Manuscript* or any consequences arising from the use of any information it contains.

1 **Enhanced visible-active photochromism of polyoxomet-**  
2 **alates/TiO<sub>2</sub> composite film by combining Bi<sub>2</sub>O<sub>3</sub> nanoparticles**

3

4 Xiansheng Wang<sup>1</sup>, Yan Sun<sup>1</sup>, Changcheng Liu<sup>2</sup>, Wei Feng<sup>1\*</sup>, Donglei Zou<sup>1</sup>

5

6 <sup>1</sup> Key Lab of Groundwater Resources and Environment, Ministry of Education,  
7 Jilin University, Changchun 130021, P. R. China

8 <sup>2</sup> Department of Aviation Oil and Materials, Air and Force Service College,  
9 Jiangsu Xuzhou, 221000, P.R.china

10

11

12 **Abstract**

13 Novel photochromic hybrid film was successfully synthesized by introducing Bi<sub>2</sub>O<sub>3</sub> into  
14 phosphomolybdic acid (PMoA)/TiO<sub>2</sub> system as visible light sensitizer. The influence of  
15 Bi<sub>2</sub>O<sub>3</sub> addition on microstructure and photochromic properties was studied via transmis-  
16 sion electron microscope (TEM), Fourier transform infrared spectroscopy (FT-IR), ultravi-  
17 olet-visible spectra (UV-vis) and X-ray photoelectron spectroscopy (XPS). Results re-  
18 vealed that Keggin geometry of PMoA and basic structure of Bi<sub>2</sub>O<sub>3</sub> were preserved in the  
19 obtained film, and the interaction between PMoA and TiO<sub>2</sub> was strengthened after com-  
20 bining Bi<sub>2</sub>O<sub>3</sub>. Upon visible light irradiation, the composite films changed from colorless to  
21 blue and showed reversible photochromism in the presence of oxygen. Moreover, pho-

1    tochromic performance of Bi<sub>2</sub>O<sub>3</sub>/PMoA/TiO<sub>2</sub> film was better than that of PMoA/TiO<sub>2</sub> film.

2    The amount of PMoA participating in photo-reductive reaction increased after adding

3    Bi<sub>2</sub>O<sub>3</sub> into PMoA/TiO<sub>2</sub> composite, which resulted in photochromic efficiencies enhancing.

4    **Keywords:** Polyoxometalates; Bi<sub>2</sub>O<sub>3</sub> nanoparticles; Visible light photochromism; Compo-  
5    site film

6

## 7    **1. Introduction**

8    Photochromic materials, whose optical absorption properties change in response to

9    light, have been the focus of intensive investigations for several decades because of

10   their potential applications in a variety of fields, such as information display, optical

11   switching, optical memories and sensors, and high-density optical storage.<sup>1-4</sup> Poly-

12   oxometalates (POMs), which usually refers to a series of multi-core inorganic met-

13   al-oxide clusters, can accept one or more electrons to yield mixed-valency colored

14   species due to their fundamental structures and versatile electronic properties.<sup>5,6</sup> Con-

15   sequently, it has become one of the most attractive photochromic materials. By en-

16   trapping POMs into inorganic or organic networks, various photosensitive systems

17   were built up and photochromic properties of materials were related to the reduction

18   potentials of POMs.<sup>7</sup> Up to now most studies on photochromism of POMs are based

19   on UV light irradiation, however, the development of photochromic materials with

20   superior visible light response is highly anticipated for the purpose of efficient utiliza-

21   tion of solar energy and common semiconductor laser sources.<sup>8,9</sup>

1 Some efforts have been made to promote the photoresponse of materials in visible  
2 light region. Ramirez confirmed that the photochromic response of  $\text{MoO}_3$  improved  
3 with the addition of CdS as a visible light sensitizer.<sup>10</sup> By depositing Au nanoparticles  
4 on the surface of  $\text{MoO}_3$  film, the Mo/Au film became more sensitive to visible light  
5 than  $\text{MoO}_3$  film.<sup>11</sup> Such a combination of the third functional phrase allowed the  
6 achievement of a new system by using visible light excitation. After that, Yao et al.  
7 reported the preparation of hybrid film fabricated from phosphomolybdic acid (PMoA)  
8 and PVP with photochromism under blue light (400-500 nm) and the absorbance can  
9 be enhanced dramatically through subsequent thermal treatment.<sup>12</sup> Embedding PMoA  
10 into appropriate inorganic system via chemical bond might fabricate novel  
11 PMoA/inorganic system which was fairly sensitive to visible light.

12 Lately, bismuth oxide ( $\text{Bi}_2\text{O}_3$ ), an inorganic semiconductor, has showed promise in  
13 the conversion of solar energy because of its visible-light response and good photo-  
14 chemical stability.<sup>13,14</sup> Especially,  $\text{Bi}_2\text{O}_3$  can provide electrons to induce the reduction  
15 of heteropolyacids (heteropolyblues generated) in the photochemical reaction. In this  
16 study, we introduce  $\text{Bi}_2\text{O}_3$  as visible light sensitizer into PMoA/ $\text{TiO}_2$  system and the  
17 photochromic properties of as-prepared films were investigated. Experimental results  
18 demonstrated that the photochromic performance of PMoA/ $\text{TiO}_2$  film has improved  
19 with addition of  $\text{Bi}_2\text{O}_3$  nanoparticles in visible light region.

## 20 **2. Experimental section**

### 21 **2.1 Materials**

1 Phosphomolybdic acid (PMoA) was purchased from Sinopharm Chemical Reagent  
2 (China) and recrystallized before use. N-butyl titanate and Bismuth nitrate [ $\text{Bi}(\text{NO}_3)_3 \cdot$   
3  $5\text{H}_2\text{O}$ ] were obtained from Tianjin Guangfu Fine Chemicals Research Institute (China)  
4 and used as received. All other chemical reagents were of analytical grade and used as  
5 received.

## 6 **2.2 Preparation**

7 2 mL N-butyl titanate was dissolved in the 10 mL absolute ethanol and stirred the  
8 mixture for 30 min. Then 2 mL acetic acid and 0.7 mL triethanolamine were added to  
9 the N-butyl titanate solution. With constant stirring for 1 h, 10 mL absolute ethanol  
10 and 0.2 mL deionized water was gradually added to the mixed solution, for 1 h stir-  
11 ring shallow yellow transparent sol was obtained. Then, 0.5 mL acetylacetone was  
12 added to the transparent sol for 30 min stirring. Finally, the transparent  $\text{TiO}_2$  sol was  
13 obtained after 24 h aging.<sup>15</sup>

14 Bismuth oxide ( $\text{Bi}_2\text{O}_3$ ) nanoparticles were fabricated hydrothermally by utilizing  
15  $\text{Bi}(\text{NO}_3)_3 \cdot 5\text{H}_2\text{O}$  (0.025 mol/L) as starting material, which was then added with 10%  
16  $\text{NH}_3\text{H}_2\text{O}$  under vigorous stirring and pH value was modified to 8.5. Then the mixture  
17 was charged into polytetrafluoroethylene-lined parr autoclave with a filling capacity of  
18 80% and hydrothermal synthesis of  $\text{Bi}_2\text{O}_3$  was conducted at  $180^\circ\text{C}$  for 12h.

19 PMoA were dissolved in ethanol with a concentration of 10 mg/mL. Then 1 mL  
20 PMoA solution was slowly dripped into the 10 mL  $\text{TiO}_2$  sol and mixed together.

21 A transparent solution was obtained by slowly adding 500  $\mu\text{L}$   $\text{Bi}_2\text{O}_3$  (2 mg/mL) etha-

1 nol solution into the mixture and vigorously stirring at room temperature for 2 h. Fi-  
2 nally, PMoA/TiO<sub>2</sub> and Bi<sub>2</sub>O<sub>3</sub>/PMoA/TiO<sub>2</sub> composite films were prepared by dripping  
3 the transparent solution on various substrates by using a 100  $\mu$ L syringe. All films  
4 were dried in a chamber with stable air humidity controlled within 60% in order to  
5 obtain optically perfect film. The thickness of hybrid film was approximately 2.2  $\mu$ m,  
6 which was measured by a FCT-103 Film Thickness Measurement System (LCD Lab,  
7 Changchun Institute of Optics, Fine Mechanics and Physics, Chinese Academy of  
8 Science).

### 9 **2.3 Instrumental analysis**

10 TEM images of samples were observed on a JEOL JEM-200CX transmission electron  
11 microscope by dripping complex solution onto copper grids. FT-IR spectra were de-  
12 termined by the samples deposited on the KBr pellets at room temperature with a Ni-  
13 colet Impact 410 FT-IR spectrometer in the wavenumber range of 2000-400  $\text{cm}^{-1}$ .

14 Absorption of all samples was measured on an UV-vis spectrophotometer (Shimadzu  
15 UV-1601PC) with 1 nm optical resolution in the range of 300-900 nm. XPS meas-  
16 urements were taken in an ESCALAB 250 photoelectron spectrometer to acquire the  
17 information on chemical binding energy of hybrid film. Photochromic experiments  
18 were carried out by using a 500 W Xe lamp as the light source and the light was  
19 passed through a glass filter ( $\lambda > 422$  nm, ZUL0422 ASAHI Co). All the measurements  
20 were carried out at room temperature.

## 21 **3. Results and discussion**

### 1 3.1 TEM measurements

2 The microstructure of the composite films was observed by TEM images. TiO<sub>2</sub> sol-gel  
3 film was uniform without particles aggregation. The PMoA particles exhibited regular  
4 spherical shape with average diameter of 60 nm in PMoA/TiO<sub>2</sub> film. As shown in  
5 Fig. 1b, Bi<sub>2</sub>O<sub>3</sub> nanoparticles were sphere with the size of 30 nm. Compared Fig. 1d  
6 with Fig. 1c, the participation of Bi<sub>2</sub>O<sub>3</sub> had no effect on morphology of PMoA in  
7 composite system except slight aggregations and Bi<sub>2</sub>O<sub>3</sub> well dispersed in the compo-  
8 site. Inset selected area electron diffraction (SAED) pattern took on samples exhibited  
9 that PMoA still maintained the single crystal structure after Bi<sub>2</sub>O<sub>3</sub> adding, which fur-  
10 ther illustrated that there was no impact on distribution of PMoA in PMoA/TiO<sub>2</sub> film  
11 by Bi<sub>2</sub>O<sub>3</sub> nanoparticles.

### 12 3.2 FT-IR spectra

13 To confirm the molecular structure and chemical bonds of films gotten from the ex-  
14 periment, comparisons of FT-IR spectra for PMoA, Bi<sub>2</sub>O<sub>3</sub>, TiO<sub>2</sub> sol-gel film,  
15 PMoA/TiO<sub>2</sub> and Bi<sub>2</sub>O<sub>3</sub>/PMoA/TiO<sub>2</sub> composite films were performed. The characteris-  
16 tic bands of TiO<sub>2</sub> appeared and verified the presence of TiO<sub>2</sub> without any decomposi-  
17 tion in the composite film. The records of spectra for PMoA of Keggin structure pre-  
18 sented four characteristic vibration bands for P-Oa, Mo-Od, Mo-Ob-Mo and  
19 Mo-Oc-Mo at 1064, 960, 867, 780 cm<sup>-1</sup> respectively.<sup>16</sup> In the composite films of  
20 PMoA/TiO<sub>2</sub> and Bi<sub>2</sub>O<sub>3</sub>/PMoA/TiO<sub>2</sub>, those characteristic bands were similar to pure  
21 PMoA with slight shifts, which demonstrated that the basic structure of Keggin ge-

ometry was still preserved.

Generally, the Mo-Od vibration was considered as a pure stretching one, whose peak position was greatly impacted by the anion-anion interaction.<sup>17</sup> The Mo-Od asymmetrical stretching frequency of PMoA/TiO<sub>2</sub> hybrid film had a red shift by 4 cm<sup>-1</sup>. This was attributed to the influence of TiO<sub>2</sub>, which led to the increase of the anion-anion distance and the weakness of anion-anion electrostatic interaction. Because  $\nu(\text{Mo-Ob-Mo})$  and  $\nu(\text{Mo-Oc-Mo})$  vibrations were not pure stretching and cannot be free from bending character, there was a competition of opposing effects. The electrostatic anion-anion interaction led to an increase of the frequencies of vibrations.<sup>16</sup> So the Mo-Ob-Mo and Mo-Oc-Mo bands can be considered as foundation to evaluate the interaction between the two inorganic components. Meantime, the bands of  $\nu(\text{Mo-Ob-Mo})$  and  $\nu(\text{Mo-Oc-Mo})$  had blue shifts by 2 and 8 cm<sup>-1</sup> respectively, which was due to the formation of Mo-O-Ti band between PMoA and TiO<sub>2</sub>.<sup>18,19</sup>

In addition, the  $\nu(\text{P-Oa})$  band had no change because there was no impact on P-Oa vibration after Bi<sub>2</sub>O<sub>3</sub> adding. Comparing with PMoA/TiO<sub>2</sub> film, the Mo-Od had red shifts and Mo-Ob-Mo and Mo-Oc-Mo had blue shifts, illustrating that Bi<sub>2</sub>O<sub>3</sub> strengthened the bonded interaction between PMoA and TiO<sub>2</sub>. Irradiated with visible light, the  $\nu(\text{Mo-Ob-Mo})$  and  $\nu(\text{Mo-Oc-Mo})$  vibration bands associated with PMoA in the composite film shifted, which should be attributed to the formation of heteropolyblues. Additionally, the presence of the characteristic vibration (at 400-600 cm<sup>-1</sup> assigned to Bi-O band) for Bi<sub>2</sub>O<sub>3</sub> were found in the composite film either with or with-



1 out irradiation.<sup>20</sup> Results revealed the Bi<sub>2</sub>O<sub>3</sub> nanoparticles were preserved during the  
2 composite process.

### 3 **3.3 Photochromic behavior**

4 The coloration process was collected by UV-vis absorption spectra of PMoA/TiO<sub>2</sub>  
5 and Bi<sub>2</sub>O<sub>3</sub>/PMoA/TiO<sub>2</sub> composites with irradiation of visible light (Fig.3a and b).

6 There was no obvious absorption before irradiation. When subjected to visible light,  
7 the colorless films turned deep blue and one broad absorption band at 730 nm was

8 detected, attributing to intervalence charge transfer (IVCT, Mo<sup>6+</sup>→Mo<sup>5+</sup>).<sup>21,22</sup> With  
9 prolonging irradiation time, the absolute absorbance of PMoA/TiO<sub>2</sub> and

10 Bi<sub>2</sub>O<sub>3</sub>/PMoA/TiO<sub>2</sub> films increased and reached saturation gradually with irradiation  
11 for 14 and 16 min respectively. For Bi<sub>2</sub>O<sub>3</sub>/PMoA/TiO<sub>2</sub> film, the intensity of absorb-

12 ance at 730 nm was 0.152 after irradiating for 16 min, which was 1.42 times stronger  
13 than that of PMoA/TiO<sub>2</sub> film under the same condition. Results indicated that Bi<sub>2</sub>O<sub>3</sub>

14 were in favor of the formation of heteropolyblues and improved the light absorption  
15 efficiency of composite film.

16 The kinetics of the coloration process was also investigated by monitoring the ab-

17 sorbance changes at 730 nm as a function of irradiation time (see Fig.4). The photo-

18 chromic process of the two retained films followed first-order kinetics with rate con-

19 stants  $k_1=0.17 \text{ min}^{-1}$  and  $k_2=0.21 \text{ min}^{-1}$  for PMoA/TiO<sub>2</sub> and Bi<sub>2</sub>O<sub>3</sub>/PMoA/TiO<sub>2</sub> film

20 respectively.

21 For the PMoA/TiO<sub>2</sub> and Bi<sub>2</sub>O<sub>3</sub>/PMoA/TiO<sub>2</sub> composite films, the similar bleaching

1 process was shown up. Fig.5 only showed the bleaching process of  $\text{Bi}_2\text{O}_3/\text{PMoA}/\text{TiO}_2$   
2 composite film. After visible light was turned off, the colored film began to bleach  
3 gradually in air. But if it was placed to avoid exposure to oxygen, such as protected by  
4 nitrogen or placed in vacuum, the color of composite film kept stable for a long time,  
5 which suggested that oxygen played an important role in the oxidation of  $\text{Mo}^{5+}$  to  
6  $\text{Mo}^{6+}$  during the bleaching process. In particular, the increase of temperature will rap-  
7 idly accelerate the bleaching process of colored film. The bleaching process finished  
8 in 30 min when heating the colored film at  $100^\circ\text{C}$ . And the photochromic reversibility  
9 of composites was quite good, as shown in Fig.6. The maximum of absorbance was  
10 almost consistent with the increasing of irradiation times.

### 11 **3.4 Photochromic mechanism**

12 Optical band gap studies have proven to be an effective tool for investigating the op-  
13 tical response of composites. The band gap energy values can be determined through  
14 the optical absorption spectra at the fundamental absorption edge of materials. Fig.7  
15 showed the UV absorbance edge of the two as-prepared films before irradiation,  
16 which reflected the influence of  $\text{Bi}_2\text{O}_3$  on the optical properties. The absorption edge  
17 of  $\text{Bi}_2\text{O}_3/\text{PMoA}/\text{TiO}_2$  had a red shift from 402 nm to 433 nm compared with  
18  $\text{PMoA}/\text{TiO}_2$  and the shift of optical response to visible region could be well under-  
19 stood from the decrease in the band gap value from 3.08 eV to 2.86 eV. This demon-  
20 strated that the addition of  $\text{Bi}_2\text{O}_3$  narrowed the band gap and improved the optic ab-  
21 sorbance performance of  $\text{PMoA}/\text{TiO}_2$  hybrid film.

1 XPS spectra were used to investigate the influence of  $\text{Bi}_2\text{O}_3$  nanoparticles on the vari-  
2 ation of electronic structure of the films during photochromic process so as to find the  
3 mechanism (as shown in Fig.8a and b). By employing Gaussian deconvolution,  $\text{Mo}_{3d}$   
4 binding energies were separated into two degenerated energy levels ( $\text{Mo}_{3d5/2}$  and  
5  $\text{Mo}_{3d3/2}$ ) and the values were listed in Table 1.<sup>23</sup> The  $\text{Mo}_{3d}$  doublet of  $\text{Mo}^{5+}$  were all  
6 detected in  $\text{PMoA}/\text{TiO}_2$  and  $\text{Bi}_2\text{O}_3/\text{PMoA}/\text{TiO}_2$  hybrid films, which indicated that the  
7 reductive reaction took place after films exposed to visible light. Compared with the  
8 binding energies of  $\text{PMoA}/\text{TiO}_2$ , the values of  $\text{Mo}_{3d5/2}$  and  $\text{Mo}_{3d3/2}$  were both lower  
9 for  $\text{Mo}^{6+}$  and  $\text{Mo}^{5+}$  by introducing  $\text{Bi}_2\text{O}_3$ . Evidently, different binding energies in  
10  $\text{Bi}_2\text{O}_3/\text{PMoA}/\text{TiO}_2$  system presented different reductive valence state during the pho-  
11 to-reduction process, which illustrated the chemical microenvironment of Mo was  
12 changed. Moreover, the  $\text{Mo}^{5+}/\text{Mo}$  ratio of  $\text{PMoA}/\text{TiO}_2$  was 0.38, much lower than that  
13 of  $\text{Bi}_2\text{O}_3/\text{PMoA}/\text{TiO}_2$  (0.49). It can be concluded that photo-reduction degree was en-  
14 hanced with participation of  $\text{Bi}_2\text{O}_3$ , which led to better photochromic response under  
15 the same irradiated condition.

16 As for the  $\text{PMoA}/\text{TiO}_2$  system, the mechanism was further interpreted according to  
17 the energy levels of the two starting materials (as shown in Fig.9a). The lowest energy  
18 excitation was from  $\text{TiO}_2$  valance band (VB) to  $\text{PMoA}$  conduction band (CB), 2.09eV  
19 through calculation, which was just located at visible light absorption range.<sup>24</sup> How-  
20 ever, the electron transfer between  $\text{TiO}_2$  VB and  $\text{PMoA}$  CB was achieved with the  
21 formation of Mo-O-Ti bond with charge transfer characteristic at the composite inter-

1 face, which was forbidden normally. Irradiated with visible light, electrons excited  
2 from TiO<sub>2</sub> valance band migrated to condition band of PMoA through Mo-O-Ti bond.  
3 And the electron transfer was promoted by Mo-O-Ti bond, consequently Mo<sup>6+</sup> was  
4 reduced to Mo<sup>5+</sup>. Thus, it can be concluded that the photo-reduction process of  
5 PMoA/TiO<sub>2</sub> composite film occurred according to electron transfer mechanism.  
6 The driving force for electron transfer between PMoA and Bi<sub>2</sub>O<sub>3</sub> was the relative en-  
7 ergy difference between the conduction band of the two starting materials (as shown  
8 in Fig.9b).<sup>25</sup> Bi<sub>2</sub>O<sub>3</sub>, a visible light sensitizer, acted as a donor providing more electrons  
9 under visible light irradiation since it is good photoresponsive materials. The bottom  
10 of conduction band for PMoA was lower than that of Bi<sub>2</sub>O<sub>3</sub>, favoring electrons arising  
11 from Bi<sub>2</sub>O<sub>3</sub> injected into the conduction band of PMoA. Heteropolyblues was pro-  
12 duced by the reaction of PMoA and the conduction-band electrons. Thus PMoA ob-  
13 tained electrons provided by both TiO<sub>2</sub> and Bi<sub>2</sub>O<sub>3</sub> and more Mo<sup>6+</sup> was reduced to  
14 Mo<sup>5+</sup>. This may be concluded as the main cause for the enhancement of photochromic  
15 properties with the addition of Bi<sub>2</sub>O<sub>3</sub>, which was in good agreement with the XPS  
16 measurements.

#### 17 **4. Conclusion**

18 Novel photochromic hybrid film sensitive to visible light was developed by combin-  
19 ing Bi<sub>2</sub>O<sub>3</sub> with PMoA/TiO<sub>2</sub> composite. The participation of Bi<sub>2</sub>O<sub>3</sub> strengthened the  
20 interaction between PMoA and TiO<sub>2</sub>. When exposed to visible light, the hybrid film  
21 turned blue in color and the photochromic process was fitted to be first-order kinetics.

1 Moreover, Bi<sub>2</sub>O<sub>3</sub>/PMoA/TiO<sub>2</sub> composite film showed better photochromic response  
2 than PMoA/TiO<sub>2</sub> film. PMoA obtained electrons provided by Bi<sub>2</sub>O<sub>3</sub> and TiO<sub>2</sub> simul-  
3 taneously during the photo-reduction process, resulting in the improvement of photo-  
4 chromic properties. This study presented the method to construct a hybrid film with  
5 visible light photochromism by the deposition of a light sensitizer and paved a novel  
6 strategy to explore composite films practically used in solar energy application.

7

## 8 **Acknowledgment**

9 The authors acknowledge the financial support from the National Natural Science  
10 Foundation of China (No.61340048) and Industrial Technology Research and Devel-  
11 opment projects in Jilin province (No.2013C044).

12

## 13 **References**

- 14 1. R.C. Shallcross, P.O. Korner, E. Maibach, A. Kohnen and K. Meerholz, *Adv. Mater.*,  
15 2013, **25**, 4807-4813.
- 16 2. Y.F. Chen, G .S. Yu, F. Li, C.F. Xie and G.P. Tian, *J. Mater. Chem. C*, 2013, **1**,  
17 3842-3850.
- 18 3. M. Singer and A. Jaschke, *J. Am. Chem. Soc.*, 2010, **132**, 8372-8377.
- 19 4. J.J. Zhang, Q. Zou and H. Tian, *Adv. Mater.*, 2013, **25**, 378-399.
- 20 5. T. He and J.N. Yao, *J. Photoch. Photobio. C*, 2003, **4**, 125-143.
- 21 6. M.T. Pope, Heteroploy and Isopolyoxometalates, *Springer-Verlag, Berlin*, 1983.

- 1 7. G.J. Zhang, Z.H. Chen, T. He, H.H. Ke, Y. Ma, K. Shao, W.S. Yang and J.N. Yao, *J.*  
2 *Phys. Chem. B*, 2004, **108**, 6944-6948.
- 3 8. L.S. Zhang, W.Z. Wang, J.O. Yang, Z.G. Chen, W.Q. Zhang, L. Zhou and S.W. Liu,  
4 *Appl. Catal a-Gen.*, 2006, **308**, 105-110.
- 5 9. X.F. Jing, D.L. Zou, Q.L. Meng, W. Zhang, F.J. Zhang, W. Feng and X.K. Han,  
6 *Inorg. Chem. Commun.*, 2014, **46**, 149-154.
- 7 10. M.A. Quevedo-Lopez, R.F. Reidy, R.A. Orozco-Teran, O. Mendoza-Gonzalez and  
8 R. Ramirez-Bon, *J. Mater. Sci-Mater. El*, 2000, **11**, 151-155.
- 9 11. T. He, Y. Ma, Y. Cao, Y.H. Yin, W.S. Yang and J.N. Yao, *Appl. Surf. Sci.*, 2001,  
10 **180**, 336-340.
- 11 12. G.J. Zhang, W.S. Yang and J.N. Yao, *Adv. Funct. Mater.*, 2005, **15**, 1255-1259.
- 12 13. R. Chen, Z.R. Shen, H. Wang, H.J. Zhou, Y.P. Liu, D.T. Ding and T.H. Chen, *J.*  
13 *Alloy. Compd.*, 2011, **509**, 2588-2596.
- 14 14. C.H. Wang, C.L. Shao, L.J. Wang, L. Zhang, X.H. Li and Y.C. Liu, *J. Colloid.*  
15 *Interf. Sci.*, 2009, **333**, 242-248.
- 16 15. C. Lu, Y. Sun, J.L. Liu, X.S. Wang, S.L. Liu and W. Feng, *J. Appl. Polym. Sci.*,  
17 2015, **132**, 41583-41589.
- 18 16. Q.Y. Wu, H.H. Lin and G.Y. Meng, *J. Solid State Chem.*, 1999, **148**, 419-424.
- 19 17. C. S. Ha, H. D. Park and C. W. Frank, *Chem. Mater.*, 2000, **12**, 839-844.
- 20 18. J. Wang, G.J. Zhang, W.S. Yang and J.N. Yao, *Acta Chim. Sinica*, 2005, **63**,  
21 1951-1956. (in Chinese)

- 1 19. R.B. Watson and U.S. Ozkan, *J Phys Chem B*, 2002, **106**, 6930-6941.
- 2 20. F. Miyaji, T. Yoko and S. Sakka, *J. Non-Cryst. Solids*, 1990, **126**, 170-172.
- 3 21. T. Yamase, *Chem. Rev.*, 1998, **98**, 307-326.
- 4 22. K. Adachi, T. Mita, S. Tanaka, K. Honda, S. Yamazaki, M. Nakayama, T. Goto  
5 and H. Watarai, *RSC Advances*, 2012, **2**, 2128-2136.
- 6 23. Z.L. Wang, R.L. Zhang, Y. Ma, L.D. Zheng, A. Peng, H.B. Fu and J.N. Yao, *J.*  
7 *Mater. Chem.*, 2010, **20**, 1107-1111.
- 8 24. S.H. Elder, F.M. Cot, Y. Su, S.M. Heald, A.M. Tyryshkin, M.K. Bowman, Y. Gao,  
9 A.G. Joly, M.L. Balmer, A.C. Kolwaite, K.A. Magrini and D.M. Blake, *J. Am. Chem.*  
10 *Soc.*, 2000, **122**, 5138-5146.
- 11 25. T. He and J.N. Yao, *Prog. Mater. Sci.*, 2006, **51**, 810-879.
- 12

## Figure Captions

**Fig.1** TEM images of (a)  $\text{TiO}_2$  sol-gel film, (b)  $\text{Bi}_2\text{O}_3$  nanoparticles, (c)  $\text{PMoA/TiO}_2$  and (d)  $\text{Bi}_2\text{O}_3/\text{PMoA/TiO}_2$  composite film.

**Fig.2** FT-IR spectra of (a)  $\text{PMoA}$ , (b)  $\text{Bi}_2\text{O}_3$ , (c)  $\text{TiO}_2$  sol-gel film, (d)  $\text{PMoA/TiO}_2$ ,  $\text{Bi}_2\text{O}_3/\text{PMoA/TiO}_2$  composite film (e) before and (f) after visible light irradiation.

**Fig.3** UV-vis spectra of (a)  $\text{PMoA/TiO}_2$  and (b)  $\text{Bi}_2\text{O}_3/\text{PMoA/TiO}_2$  composite film.

**Fig.4** The kinetic plot of the photochromic process for  $\text{PMoA/TiO}_2$  and  $\text{Bi}_2\text{O}_3/\text{PMoA/TiO}_2$  composite film.

**Fig.5** Bleaching process of  $\text{Bi}_2\text{O}_3/\text{PMoA/TiO}_2$  composite film after irradiation.

**Fig.6** The absorbance change at 730 nm of  $\text{Bi}_2\text{O}_3/\text{PMoA/TiO}_2$  hybrid film during repeated coloration-decoloration process.

**Fig.7** UV absorbance edge of  $\text{PMoA/TiO}_2$  and  $\text{Bi}_2\text{O}_3/\text{PMoA/TiO}_2$  hybrid film.

**Fig.8** Gaussian deconvolution of  $\text{Mo}_{3d}$  level spectra of (a)  $\text{PMoA/TiO}_2$  and (b)  $\text{Bi}_2\text{O}_3/\text{PMoA/TiO}_2$  composite film after irradiation.

**Fig.9** (a) Arrangement of the  $\text{PMoA}$  and  $\text{TiO}_2$  valance bands (VB) and conduction bands (CB) for  $\text{PMoA/TiO}_2$  composite film. (b) Schematic presenting the electron transfer between  $\text{PMoA}$  and  $\text{Bi}_2\text{O}_3$ .



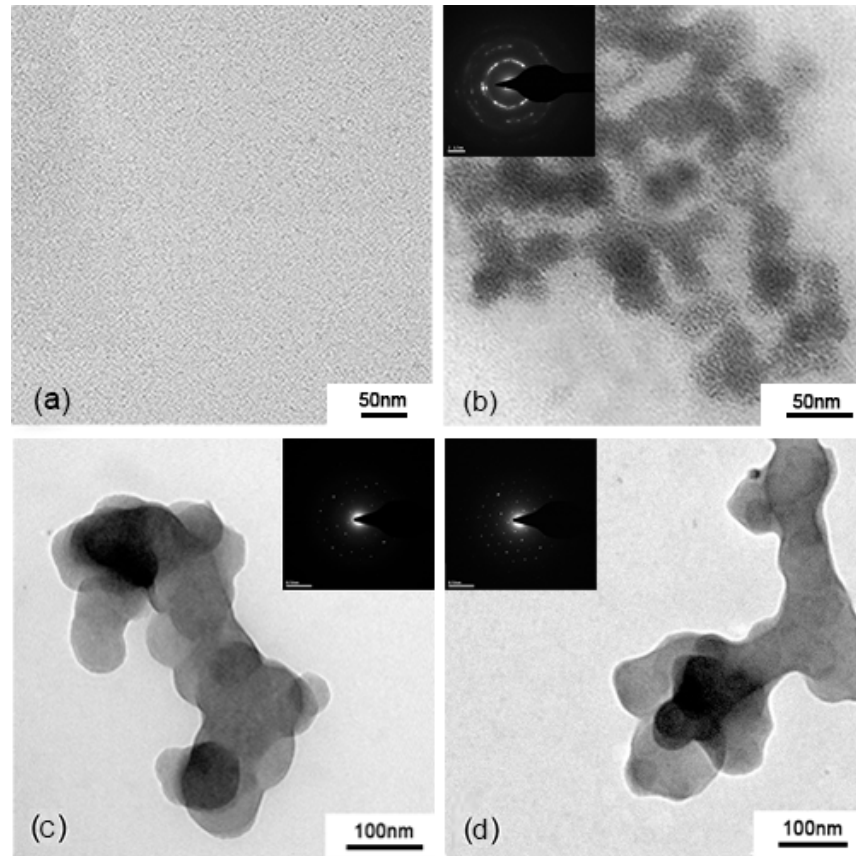
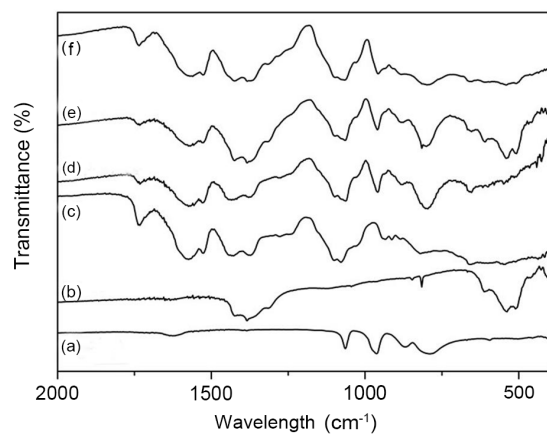
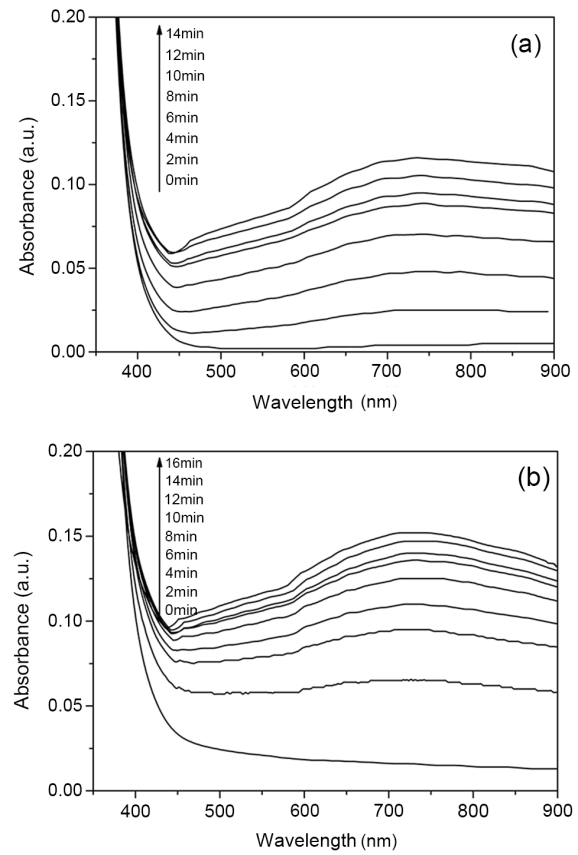


Fig.1

**Fig.2**

**Fig.3**

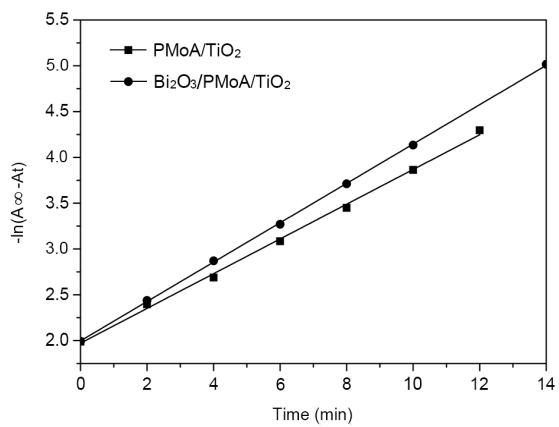
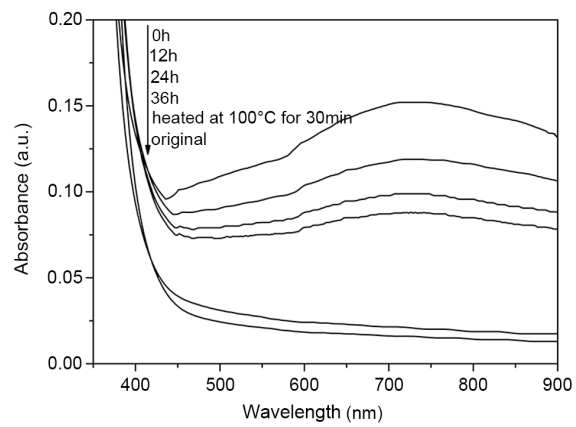
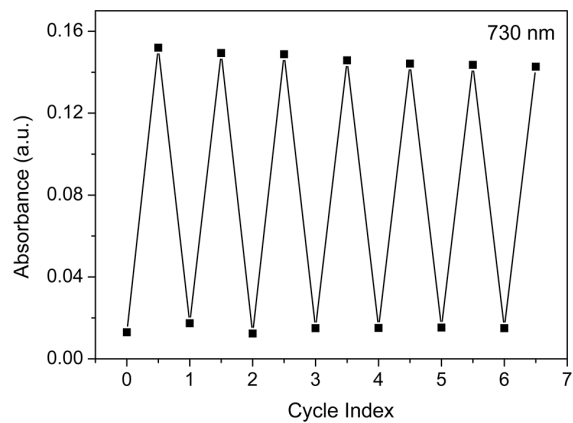
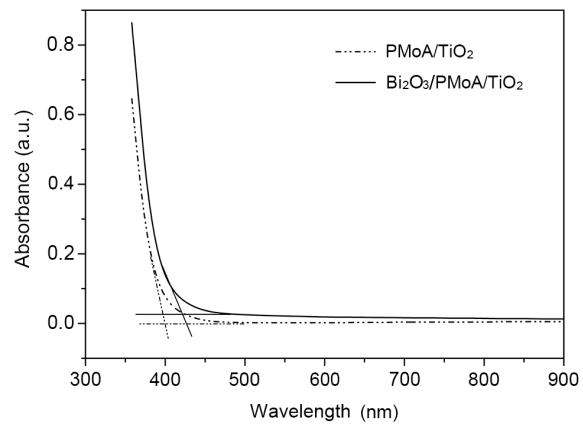
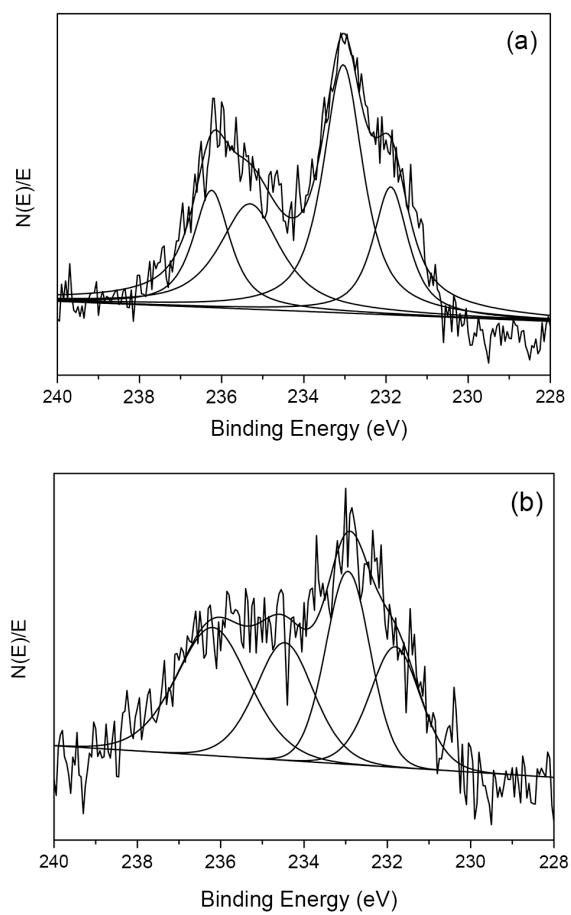


Fig.4

**Fig.5**

**Fig.6**

**Fig.7**

**Fig.8**



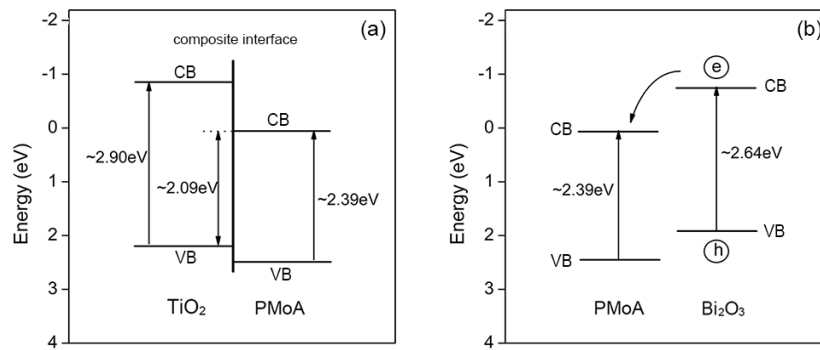


Fig.9

**Table 1** Binding energies of Mo<sub>3d</sub> energy level and Mo<sup>5+</sup>/Mo ratios of PMoA/TiO<sub>2</sub> and Bi<sub>2</sub>O<sub>3</sub>/PMoA/TiO<sub>2</sub> composite film after irradiation.

Sample	Mo <sup>5+</sup>		Mo <sup>6+</sup>		Mo <sup>5+</sup> /Mo Ratios
	3d <sub>3/2</sub>	3d <sub>5/2</sub>	3d <sub>3/2</sub>	3d <sub>5/2</sub>	
PMoA/TiO <sub>2</sub>	235.31	231.88	236.25	233.04	0.38
PMoA/TiO <sub>2</sub> /Bi <sub>2</sub> O <sub>3</sub>	234.46	231.71	236.19	232.94	0.49